LAWRENCE
LIVERMORE
NATIONAL
LABORATORY

UCRL-PROC-232827

MULTISCALE MODELING OF POLYMER NANOCOMPOSITES

Amitesh Maiti

July 18, 2007

2007 SAMPE Fall Technical Conference
Cincinnati, OH, United States
October 29, 2007 through November 1, 2007

MULTISCALE MODELING OF POLYMER NANOCOMPOSITES

Amitesh Maiti
Lawrence Livermore National Laboratory, Livermore, CA 94551

ABSTRACT

Polymer Nanocomposites are an important class of nanomaterials with potential applications including but not limited to structural and cushion materials, electromagnetic and heat shields, conducting plastics, sensors, and catalysts for various chemical and bio processes. Success in most such applications hinges on molecular-level control of structure and assembly, and a deep understanding of how the overall morphology of various components and the interfaces between them affect the composite properties at the macroscale. The length and time-scales associated with such assemblies are prohibitively large for a full atomistic modeling. Instead we adopt a multiscale methodology in which atomic-level interactions between different components of a composite are incorporated into a coarse-grained simulation of the mesoscale morphology, which is then represented on a numerical grid and the macroscopic properties computed using a finite-elements method.

1. INTRODUCTION

There are a large number of interesting problems in soft condensed matter that occur at length and time-scales intermediate between the atomistic scale and the macroscopic continuum. Examples include polymer adsorption, polymer-surfactant interaction, microphase separation of block copolymers, formation and coalescence of droplets in emulsion, transport through living cells, and formation of polymer networks, to name just a few. Such problems cannot be directly addressed by either conventional atomic-level molecular dynamics, or by finite-elements based continuum mechanics. Rather, one needs to take recourse to computational techniques at the intermediate scale, called the *mesoscale*.

Over the last few years several different approaches have been developed to address problems at the mesoscale. Broadly speaking, there are two distinct classes of methods - a particle-based method, as exemplified by Dissipative Particle Dynamics (DPD) (1), and a density-based method, as implemented, e.g., in the code Mesodyn (2). Traditionally, both these methods have been used to predict morphology of polymers and block copolymers in solutions, melts, and blends, and how they change under the influence of surfactants, temperature, and shear. In the present paper we summarize the use of the first approach, i.e., DPD in studying miscibility and phase-separation in composites of polymer and carbon nanotubes (CNTs). The paper is organized as follows. Section 2 gives a brief overview of our efforts to describe polymer-CNT interaction at the atomic level and point out why a coarse-grained description is necessary to describe a composite. In section 3 we provide a brief introduction to the DPD formalism and mention some small modifications made to describe the stiffness of the CNTs. In section 4 we

study the problem of miscibility of CNT and the PMMA polymer, and explore how the miscibility changes as a function of tube diameter, chemical functionalization, and the application of an external shear. In section 5 we study the patterns formed by CNTs when mixed with a block co-polymer. We then map these patterns onto a finite-element grid and compute electrical conductivity of the nanocomposite system using a finite-element method. Finally in section 6 we briefly outline a multiscale strategy for a materials problem where we attempt to create complex filler particles consisting of Palladium nanoclusters coated with multifunctional polyhedral Silsesquioxane (POSS) cages.

2. CNT-POLYMER INTERACTION – ATOMISTIC MODELING

Our interest in the problem of CNT-polymer interactions was driven by some interesting experiments performed a few years ago at Trinity College, Dublin (3). In this study different loading fractions of a powder of single-walled CNTs prepared by the arc discharge method were added to polymer-toluene solution. The polymer used was a modified form of PPV, i.e., poly(*m*-phenylenevinylene-co-2,5-dioctyloxy-*p*-phenylenevinylene), hereafter referred to as PmPV. The composite suspensions were sonicated for several minutes in a low-power sonic bath and then allowed to settle for a number of days. The resulting suspension, decanted from any settled solid, was shown to be stable over indefinite periods. Raman studies indicated that the polymer-tube system increases the frequency of the modes by 21 cm^{-1} compared to 14 cm^{-1} for tube-tube interactions. From a knowledge of the frequency of the radial breathing modes as a function of tube diameter it was inferred that the polymer interacts strongly with nanotubes within a narrow diameter range of 1.3 – 1.5 nm and weakly with tubes of other diameters. It should be noted that above 2% loading fraction, this selection process disappears. It is also dependent on the concentration of polymer in toluene. If the concentration is too high, the polymer aggregates and inhibits the polymer-CNT interaction. From initial STM observations it was suggested that the polymer wraps around the CNT in a helical fashion by following the helical hexagonal rows on the CNT surface. However, more detailed STM images revealed that in most cases there is apparently no such ordered wrapping pattern (4).

To gain theoretical insight into the nature of polymer-CNT interaction we performed molecular modeling of the PmPV-CNT system. We found that the backbone reorganizes into a relatively flat helical structure due to *meta*-phenylene linkage and repulsive interactions between the octyloxy groups. These groups are projected outwards from the helical structure. In contrast, when one octyloxy group per repeat unit is replaced by a methoxy group, the backbone prefers to remains straight, and does not reorganize into a helical structure. The polymer, in this geometry, does not expose the conjugated backbone because the octyloxy groups are projected outwards under a 45 degree angle. The exposure of the backbone plays an important role in facilitating strong induced dipolar binding between polymer and nanotube. The PmPV backbone can then easily π stack onto the nanotube. It is for this reason that PmPV with two octyloxy groups can hold nanotubes in solution, whereas PmPV with one octyloxy group is not able to do this.

Atomistic molecular dynamics simulations using the COMPASS Forcefield (5) indicate that the PmPV conformation changes due to interactions with the nanotubes. Full (computational) details are described elsewhere (6). Simulation suggests that the polymer backbone provides the strongest binding (109 kJ/mol per PmPV repeat) to the nanotubes and not the side groups. The

binding energy of the octoloxy side chains is significantly lower (50 kJ/mol per sidechain). Thus the side chains have a much greater freedom of movement. In addition, our calculations show that it is energetically more favorable for the polymer to lie along the parallel axis (Figure 1) instead of mapping the chiral angle of the tubes. However, to explain why the PmPV polymer displays preferential affinity for CNTs within a narrow range of diameters, one needs to consider not only CNT-polymer interaction, but CNT-CNT and polymer-polymer interactions. In particular, the CNT-CNT interaction is a strong function of the CNT diameter, and this fact will be utilized in a mesoscale explanation of the affinity in question, as will be seen section 4.

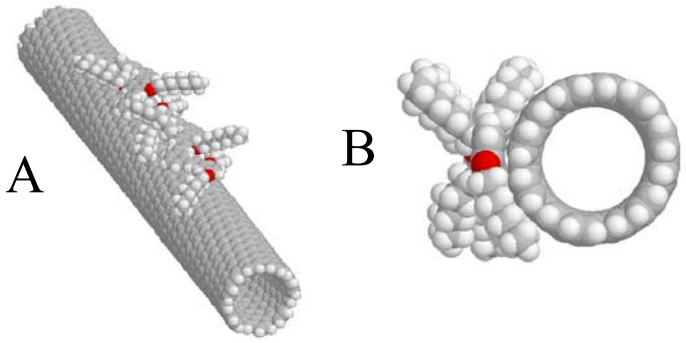

FIGURE 1. PmPV polymer (4 repeat units) on a (12,7) carbon nanotube. (A) top view and (B) side view. Carbon, hydrogen and oxygen atoms are shown in grey, white and red, respectively.

Although an atomic-level analysis provides useful insight into the interaction of individual polymer strands with an individual CNT, for a CNT-polymer nanocomposite it is important to understand the distribution of various components in the mix. Unfortunately, the length-scale and time-scale over which such a structural evolution occurs is currently beyond the scope of molecular-level modeling, and a mesoscale representation is more appropriate. In the next section we describe the basics of the mesoscale method we adopted for the CNT-polymer composite problem, i.e., Dissipative Particle Dynamics (DPD).

3. DPD – AN INTRODUCTION

In DPD (1), one represents a group of atoms (typically entire functional groups) by a single bead, thereby substantially reducing the number of particles to be simulated. The positions and velocities of the spherical beads are propagated by standard integrators as in regular MD methods and thermally equilibrated through a Langevin thermostat. But rather than interact through Lennard-Jones forces, the beads feel a simple soft pair-wise conservative potential which embodies the essential chemistry of the system. This force is short range and has a simple analytic form resulting in fast computation per time-step. More importantly it provides an effective time-step of several picoseconds, 3-4 orders of magnitude larger than typical time-steps employed in a MD simulation.

In the basic DPD formalism, the force $\vec{f}_i$ on bead *i* contains three parts, each of which is pairwise additive:

$$\vec{f}_i = \sum_j{}' (\vec{f}_{ij}^{\,c} + \vec{f}_{ij}^{\,D} + \vec{f}_{ij}^{\,R}).$$

The chemistry of mixing and segregation is governed by the term f_{ij}^{c}, which is modeled as a soft repulsion between beads *i* and *j*. It is a function of the relative separation between the beads and act along the line joining the two beads, thus being conservative (i.e. momentum conserving). Groot and co-workers (1) have established a relation between the interaction parameters describing the f_{ij}^{c} term and the Flory-Huggins χ-parameter for beads *i* and *j*. Basically, the repulsion is proportional to an interaction parameter a_{ij} , and it is the excess interaction $\Delta\bar{a} = (\bar{a}_{AB} - \bar{a}_{AA})$ that determines whether components A and B will mix or segregate. The other two terms f^D and f^R are dissipative and random forces respectively, which in tandem act as a thermostat and result in fast equilibration to the Gibbs-Boltzmann canonical ensemble.

In the basic Groot-Warren theory, all the three interaction terms described above have the same finite range R_c, which sets the basic length-scale of the system, and is defined as the side of a cube containing an average number of $\bar{\rho}$ beads. Therefore $R_c = (\bar{\rho}\, V_b)^{1/3}$**,** where V_b is the volume of a bead. One can think of $\bar{\rho}$ as a dimensionless bead-density, related to the average bead-density $\rho = 1/V_b$ by the equation $\bar{\rho} = \rho R_c^{\,3}$. Even in a heterogeneous system consisting of several different species, the basic assumption is that all bead-types (each representing a single species) are of the same volume V_b. This assumption is necessary in order to conform to the Flory-Huggins χ-parameter theory.

In addition to the three forces described above, polymeric systems also require extra spring-like interactions to describe covalent "bonding" between consecutive beads in a polymeric chain. In the commercial version of DPD (7) Hookean spring potentials have traditionally been used:

$$E_{ij} = \frac{1}{2} k^B \bar{r}_{ij}^{\,2},$$

where the energy is dependent only on the separation of the beads $\bar{r}_{ij}$ (expressed in reduced units, i.e., $\bar{r}_{ij} = r_{ij}/R_c$) and leads to a force $F_{ij} = k^B \bar{r}_{ij}$, where k^B is the force constant. This scheme has been shown to successfully reproduce the end-point distribution and exhibit the correct scaling laws for chains as short as L=10, although a microscopic theory mapping the detail of the polymer to the DPD strings has not so far been developed. For k^B it appears sufficient to use a value that does not allow excessive stretching of the bond; k^B = 4.0 has often been used and was used here for bonds in all polymer chains in the polymer-nanotube composite models. It should be noted that although the minimum bond energy is achieved for r_{ij}=0, overlapping of the beads is prevented by the soft repulsive bead-bead interaction, which works against this. There are no 1-2 or 1-3 exclusions from the soft repulsive interaction for bonded DPD beads. To represent the semi-flexible rod-like rigidity of CNTs we also added an angle dependent potential. This term is represented by a standard cosine bond angle expression as follows (8):

$$E_{ijk} = \frac{1}{2} k^{\theta} (1 + \cos\theta_{ijk}) .$$

4. CNT-PMMA COMPOSITES: DPD MODELING

One of the first major commercial application areas of Nanotechnology is turning out to be composites in which nanomaterials are dispersed within matrices of ceramics and polymers. Inclusion of even small amounts of nanomaterial coupled with appropriate processing steps appears to significantly improve mechanical, elastic, thermal, and electrical properties of composites. One specific area that has received a lot of recent attention is composite materials, in which carbon nanotubes (CNTs) are dispersed within polymeric matrices. Applications can range from structural materials, electromagnetic and heat shielding, to optoelectronics. The overall properties of CNT-polymer composite material depend on the uniformity of CNT dispersion and the degree of parallel alignment within the polymeric matrix, the efficacy of interfacial bonding between the two systems, and the way in which the above properties depend on the nanotube diameter, chirality, and functionalization of the CNT surface with organic functional groups. Since it is difficult to control many of these properties experimentally, modeling and simulations could provide crucial insight and guide further experimental effort.

With the availability of forcefields and interatomic potentials that describe CNT-polymer interaction with reasonable accuracy, it is tempting to perform classical molecular dynamics (MD) simulations. However, modeling such composites in full atomistic detail is rather challenging because even the smallest representative model involves a significant number of atoms, and more importantly the equilibration times are usually several orders of magnitude longer than a nanosecond, the typical limit of classical MD simulations. As described below, we circumvent the problem by coarse-graining both the polymer and the CNT into strings of beads, connected by Hookean springs (see section 3), and using DPD to hydrodynamically equilibriate such coarse-grained morphology.

The chemistry of polymer-nanotube interaction is incorporated through relating the DPD bead-bead repulsion to the Flory-Huggins χ-parameter (9, 10), which in turn is obtained by squaring the difference of pure-component solubility parameters (δ). The latter is defined as the square root of the cohesive energy density. Reliable average values of δ for long-chain polymers can be estimated from simple correlation methods (11, 12). On the other hand, carbon nanotubes are not polymers in the conventional sense. Nevertheless, since CNTs tend to form close-packed bundles, a good measure of their cohesive energy can be obtained from the debundling energy, *i.e.*, the energy cost of isolating a CNT from a bundle. Computing such energy with the Universal Forcefield (13), normalizing per unit volume, and taking the square root results in a solubility parameter that is essentially independent of the CNT chiral angle, and that decreases smoothly as a function of the CNT diameter (approximately as inverse square root), as shown in Fig. 2. From a simplistic interpretaion of Flory-Huggins theory we can expect that components with close enough δ, which leads to small DPD repulsion, should mix, while components with significantly differing δ should segregate.

With the above reasoning, Fig. 2 immediately provides a justification for why the PmPV polymer shows a preferential affinity for CNTs of diameters in the range ~ 1.3-1.5 nm (see

section 2). In addition, Fig. 2 suggests that PMMA polymers should mix well with CNTs of diameters close to 1.4 nm (*e.g.* (10, 10) CNTs), while PP is expected to form uniform composites with CNTs of diameters in the neighborhood of 1.9 nm (*e.g.* (15, 15) CNTs).

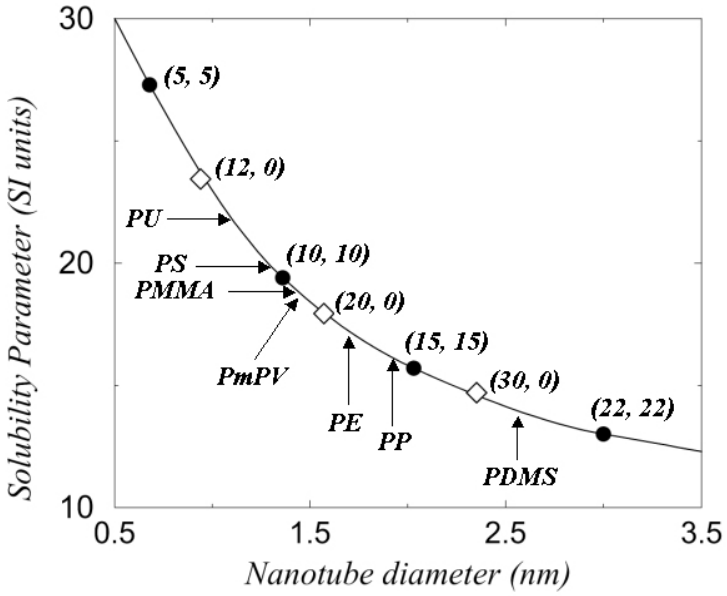

FIGURE 2. Computed solubility parameter (δ) of CNTs as a function of tube diameter. For comparison, the δ of various polymers (11) are also indicated.

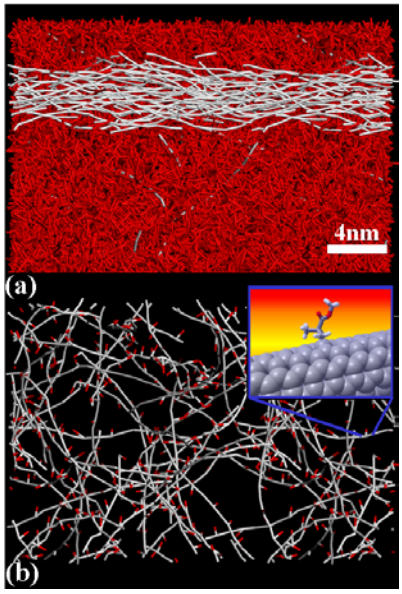

FIGURE 3. Equilibrium morphologies of (15,15) CNT-PMMA composites at ambient temperature and pressure as modeled by DPD. CNTs are shown in white in both images. In (a) the PMMA chains are shown in red while in (b) they are hidden for clarity. (a) unfunctionalized (15,15) CNTs which quickly segregate and align. (b) dispersion of (15, 15) CNTs functionalized with 30% (by volume) acrylate groups attached at regular intervals (shown in red). (b-inset) an atomistic representation of one of the acrylate groups attached to a CNT.

The above expectations are borne out in direct DPD simulations. Thus (10, 10) CNTs are found to disperse well in PMMA, although in a somewhat random orientation. Application of an external shear is found to induce more parallel alignment of the CNTs (8, 14). In contrast, the (15, 15) CNTs are found to segregate and form CNT-bundles (Fig. 3(a)). However, attachment of appropriate functional groups can render such CNTs soluble, as illustrated in Fig. 3(b) through the attachment of PMMA monomers at regular intervals of the (15, 15) CNT.

In our DPD simulations each bead (CNT or polymer) was chosen to represent the equilibrium volume of a PMMA monomer (180 $Å^3$), implying approximately 12 nm length of the simulated CNTs. We used a CNT loading fraction of 5%. The total simulation cell, if represented atomistically, would correspond to a system of $1.6x10^6$ atoms, while the total simulation time of $5x10^5$ steps corresponds to a real time of ~ 9 μs. The above clearly demonstrates the strength of mesoscale modeling in accessing much bigger length- and especially much longer time-scales than possible with standard classical molecular dynamics.

5. CNT COMPOSITE WITH DIBLOCK-COPOLYMER – PROPERTY COMPUTATION WITH FINITE-ELMENTS

The purpose of the previous application was essentially to show that a mesoscale modeling technique like DPD can be applied to study the problem of dispersion and alignment of flexible rod-like objects such as CNTs in a polymer matrix, and how the dispersion could be influenced by attaching organic functional groups and the application of an external shear. However, once the mesoscale morphology is generated, it would be useful to be able to estimate important material properties of the nanocomposite. To this end, we have recently mapped the DPD morphology of a nanocomposite onto a finite-element grid and computed properties using a finite-element method (FEM).

For clarity we wanted to investigate a property where the presence of CNTs makes a significant difference. One such property is the electrical conductance, which, for a pure metallic CNT is many orders of magnitude higher than that of a typical polymer. However, to make a polymer-CNT composite conducting it is necessary to have a conducting path from one end of the sample to the opposite end, which implies a percolating network of CNTs. The percolation problem of rigid rods and sticks has previously been investigated both analytically and through simulations. An important result from such simulations is that the critical volume fraction (CVF) corresponding to the percolation threshold is inversely proportional to the rod's aspect ratio a, implying that for CNTs (with typical $a \sim 10^3$-10^4) the CVF should be within a few tenths of a percent. Our aim was to re-visit the above problem by incorporating two more realistic materials features: (1) CNTs are not completely rigid, but possess some bending flexibility, and (2) in a multi-component polymer/fluid environment CNTs can display preferential segregation in one component over others, including the tendency to form bundles with other CNTs. Both these features can potentially affect the CVF and hence lead to interesting behavior in the electrical and thermal conductivity.

With the specific aim of lowering the CVF of CNT as compared to a completely random CNT-network, we thought of investigating CNT composites of block-copolymer systems. This is because block copolymer composition can be controlled to self-assemble a variety of phases:

lamellar, bicontinuous, gyroid and discrete micelles (15 and references therein). Thus, the hope was that with appropriate choice of polymers more structured arrangements with improved percolation of CNTs at low fractions might be possible.

The overall idea was to use DPD to compute the equilibrium distribution of various components (CNT, polymer, fluid) in the computational cell, and then to compute electrical and thermal conductivity using a finite-element modeling (FEM) approach (16) as implemented in the MesoProp software (17). In such an approach, the bead positions of DPD morphology are first converted into a concentration gradient. This is numerically mapped onto an FEM grid of homogeneous volume elements, the local properties of which are calculated from the fraction of each component phase and its assigned pure component property value. This approach has largely been applied to the calculation of thermoelastic properties of composites, including CNT-reinforced polymers. Electrical conductivity can equally well be evaluated for the composite by solving the Laplace equation:

$$\nabla.\{\sigma(\vec{r}).\nabla\varphi(\vec{r})\} = 0\,,$$

where $\sigma(\vec{r})$ and $\varphi(\vec{r})$ are the local conductivity and the local electrostatic potential respectively. MesoProp uses an algorithm in which an electric field is applied in the three main directions to the finite element mesh, and then the electrostatic energy of the composite is minimized with a conjugate gradient method.

Use of the FEM model requires a suitable choice of pure component conductivities as input. The disparity in electrical conductivity (σ) of metallic CNTs and polymer is can be almost 20 orders of magnitude with, 10^6 Sm^{-1} for CNTs compared to 10^{-13} Sm^{-1} for regular insulating polymers. Given that even for a percolating CNT network the electrical conductivity can be somewhat limited by CNT-CNT contact resistance (15), we chose a CNT:polymer conductivity ratio of 10^{10}. Since the morphology constantly evolves during simulation, a time average of representative configurations over long simulation runs (200000 steps or more) was used to generate the in-plane conductivity of the slab. This averaging is especially important around the CVF of CNTs where the percolation network continuously makes and breaks as a function of time.

The system we explored in some detail was the dispersion of CNTs in diblock copolymers of the form A_nB_{N-n}, where N is the polymer length in units of DPD beads (chosen to be 20 for concreteness and computational convenience) and n is an integer between 0 and N (inclusive). To ensure the most distinct pattern formation as a function of n, A and B must be highly immiscible. We are also most interested in the case in which the CNTs disperse preferentially into one of the polymers, allocated as the A polymer. With specific interaction parameters consistent with the above physical choices, i.e., $\Delta a_{A\text{-}B} = 20$, $\Delta a_{A\text{-}N} = 0$, $\Delta a_{B\text{-}N} = 10$ (and self-interactions $\Delta a_{A\text{-}A} = \Delta a_{B\text{-}B} = \Delta a_{N\text{-}N} = 0$), DPD simulations were performed for different values of n and different CNT fractions (limited to a few percent). Fig. 4 summarizes the results for a fixed CNT fraction (0.75% by volume) as a function of n. The left pane shows a few representative configurations from the simulations, while the right pane plots the electrical conductivity of these structures averaged over the whole trajectory of 200000 steps. The conductivity is expressed as a ratio to the conductivity computed in a pure A-polymer (i.e. n=20) for the same CNT fraction and an interesting non-monotonic structure as a function of n results. A physical explanation for such behavior is provided in ref. (15).

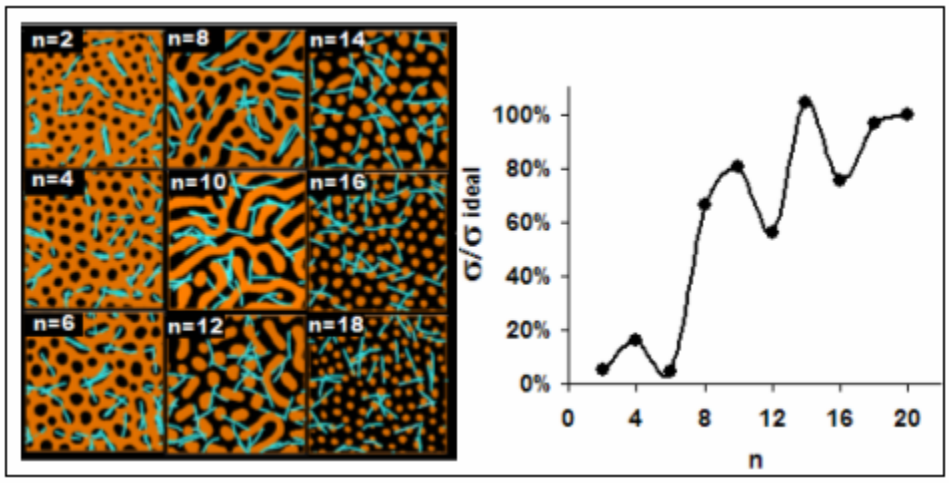

FIGURE 4. Plot of typical morphologies for 0.75 vol% CNTs in $A_nB_{(20-n)}$ block co-polymers. Polymer density fields shown using white/black (A material) and blue/orange (B material). Instantaneous positions of the CNTs beads are shown in red/cyan. Morphologies were generated using $\Delta a_{A\text{-}B}$=20, $\Delta a_{N\text{-}B}$=10, $\Delta a_{N\text{-}A}$=$\Delta a_{N\text{-}N}$=$\Delta a_{A\text{-}A}$=$\Delta a_{B\text{-}B}$=0.

6. Pd/POSS MULTIFUNCTIONAL NANOPARTICLES

In this final section we present sketches of our plans for multiscale modeling in a different system, i.e., in which Pd nanoparticles are coated with multifunctional polyhedral Silsesquioxane (POSS) cages (18) (Fig. 5). Such a system, being considered as filler particles in polymeric matrices, is supposed to perform multiple functions in addition to the customary function of enhancing mechanical properties. In the initial stages of this project we are studying the formation of the Pd/POSS system in a solvent medium. For this we are considering a multiscale modeling approach in which: (1) classical atomic-level molecular dynamics is used to compute the diffusion constant of Pd and POSS particles within the solvent; (2) a Monte Carlo algorithm (e.g., Blends ()) is used to compute binary mesoscale interaction between Pd, POSS, and the solvent; (3) the mesoscale interactions (step 2) and knowledge of diffusion constant (step 1) is used to perform DPD simulations of the evolution of particle morphology over realistic time-scales; and (4) finite-elements is used to compute useful materials properties of the appropriate composite systems.

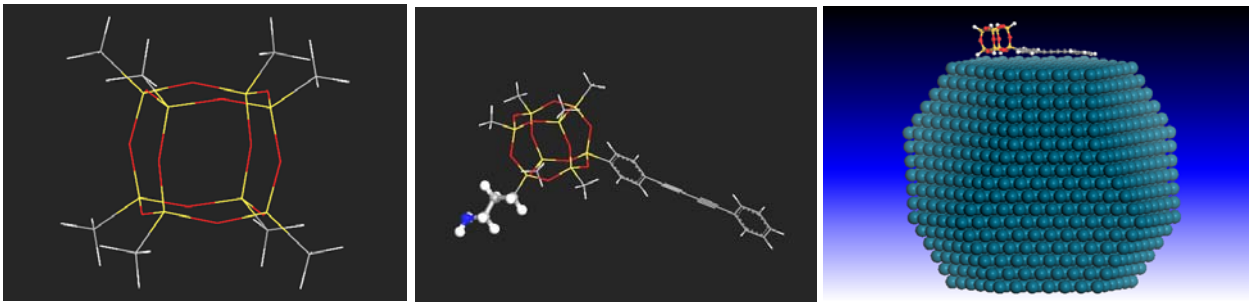

(a) (b) (c)

FIGURE 5. (a) A POSS cage; (b) Examples of different functional groups that can be attached to the corners of a POSS cage; (c) A Pd nanoparticle with realistic morphology, with a multifunctional POSS on its surface.

7. ACKNOWLEDGEMENT

The work presented here is a result of close collaborations with James Wescott, Paul Kung, Gerhard Goldbeck-Wood, and Marc In-het Panhuis. The work at LLNL was performed under the auspices of the U. S. Department of Energy (DOE) by the University of California, Lawrence Livermore National Laboratory (LLNL) under Contract No. W-7405-Eng-48, and supported in part by the project 06-SI-005 (Transformational Materials Initiative) funded by the Laboratory Directed Research and Development Program at LLNL.

8. REFERENCES

1. R. D. Groot and P. B. Warren, J. Chem. Phys. , 107, 4423 (1997).
2. J.G.E.M. Fraaije, et al., J. Chem. Phys., 106, 4260 (1997).
3. A. B. Dalton, C. Stephan, J. N. Coleman, B. McCarthy, P. M. Ajayan, S. Lefrant, P. Bernier, W. J. Blau, and H. J. Byrne, J. Phys Chem B **,** 104, 10012 (2000).
4. M. in het Panhuis, A. Maiti, J.N. Coleman, A.B. Dalton, B. McCarthy and W.J. Blau, AIP Cof. Proc., 591, 497 (2001).
5. H. Sun, J. Phys. Chem. B**,** 102, 7338 (1998).
6. M. in het Panhuis, A. Maiti, A. B. Dalton, A. van den Noort, J. N. Coleman, B. McCarthy, and W. J. Blau, J. Phys. Chem. B, 109, 478 (2003).
7. See: http://www.accelrys.com/products/mstudio/modeling/polymersandsimulations/dpd.html .
8. A. Maiti, J. Wescott, and G. Goldbeck-Wood, Int. J. Nanotechnology, 2, 198 (2005).
9. P. J. Flory, Principles of Polymer Chemistry, Cornell University Press (1953).
10. M. Doi, Introduction to Polymer Physics, Chapter 2, Clarendon Press, Oxford (1996).
11. J. Bicerano, Prediction of Polymer Properties, 2nd Ed, Pg 108-136, Marcel Dekker Inc. (1996) as implemented in Accelrys' SYNTHIA code (12). The polymer solubility parameters of Fig. 2 were computed as an average of the Fedors and van Krevelen solubility parameters as defined in this reference.
12. See: http://www.accelrys.com/cerius2/synthia.html .
13. A. K. Rappe, C. J. Casewit, K. S. Colwell, W. A. Goddard-III, and W. M. Skiff, J. Am. Chem. Soc. **,** 114, 10024 (1992).
14. A. Maiti, J. Wescott, and P. Kung, Mol. Sim., 31, 143 (2005).
15. J. Wescott, P. Kung, and A. Maiti, Appl. Phys. Lett , 90, 033116 (2007).
16. A. A. Gusev, Macromolecules , 34, 3081 (2001).
17. http://www.accelrys.com/products/mstudio/modeling/polymersandsimulations/mesoprop.html .
18. A. Maiti, R. Gee, R. Maxwell, and A. Saab, Chem. Phys. Lett. , 440, 244 (2007).